Proc. 13th International Beam Instrumentation Conference,Beijing JACoW Publishing
ISBN: 978-3-95450-249-3 ISSN: 2673-5350 doi: 10.18429/JACoW-IBIC2024-TUP30

# DEVELOPMENT OF HIGH-PRECISION BEAM POSITION MONITOR FOR THE KOREAN 4GSR PROJECT

S.W. Jang†, D. Shin, S. Ahn, D. Kim, B. Shin, Pohang Accelerator Laboratory, Pohang, South Korea



*Abstract*

The Korean 4GSR project is currently under construction in Ochang, South Korea, with the aim of achieving first beam commissioning in 2027. Designed to achieve an emittance approximately 100 times smaller than that of third-generation synchrotron radiation storage rings, the project requires the development of several high-precision beam diagnostic devices. In particular, the beam position monitor is aimed at reducing longitudinal wake impedance to suppress heating and beam instability. This paper discusses the development of two types of 4GSR BPM pick-up antennas: one utilizing a $SiO_2$ glass insulator and another designed in a cone shape using $Al_2O_3$. We will also describe the performance of these designs through beam tests. Additionally, this paper provides an overview of the current development status of the BPM system for the 4GSR project.

## DEVELOPMENT OF 4GSR BPM PICK-UP

Two types of beam position monitor (BPM) pickup antennas have been developed for the 4th generation storage ring (4GSR) project [1, 2]. The first type uses a $SiO_2$ glass insulator with a low dielectric constant, which shifts the frequency range of the longitudinal wake impedance generated by the BPM to higher frequencies. This helps reduce overall thermal loss in the BPM and allows for cleaner signal acquisition. The second type features a cone-shaped design using $Al_2O_3$, which, despite its higher dielectric constant of 9.9, has been optimized to perform at the same level as the $SiO_2$ BPM. These designs have been optimized through extensive 3D simulations to minimize ringing signals while achieving high beam position resolution [3]. The $SiO_2$ BPM consists of molybdenum pins and a $SiO_2$ glass insulator with a dielectric constant of 4, housed in ASTM-F15 material. In contrast, the $Al_2O_3$ BPM features titanium pins and a ceramic disc with a dielectric constant of 9.9, enclosed in an SUS316 stainless steel housing. Figure 1 shows that the developed two different type of 4GSR BPM sectional view for $SiO_2$ and $Al_2O3$ insulators.

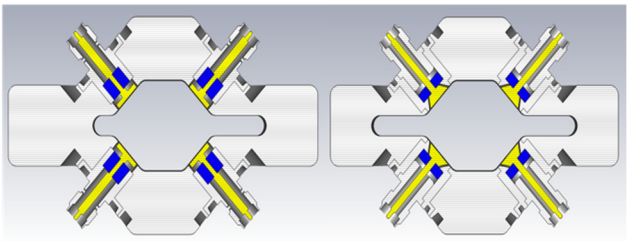

Figure 1: Development of 4GSR BPM pick-up antennas. $SiO_2$ glass BPM (left) & $Al_2O_3$ BPM (right).

† siwon@postech.ac.kr

## TDR MEASUREMENT OF 4GSR BPM PICK-UP ATNENNA

Time Domain Reflectometry (TDR) is a powerful technique used to measure the impedance along the BPM structures. By sending a fast-rise time pulse along the transmission line and measuring the reflections, we can accurately determine the characteristic impedance and detect any discontinuities in the line.

The TDR measurement provides a direct way to calculate the capacitance of the BPM structures. The relationship between the impedance $Z(t)$ and the reflection coefficient $\Gamma(t)$ is given by Eq. 1:

$$\Gamma(t) = \frac{Z(t)-Z_0}{Z(t)+Z_0}, \quad (1)$$

where $Z_0$ is the characteristic impedance of the transmission line. Figure 2 shows the TDR simulation results of the two types of BPM pick-up antennas for 4GSR, as well as the actual TDR measurement results of the prototype BPM pick-up antenna samples.

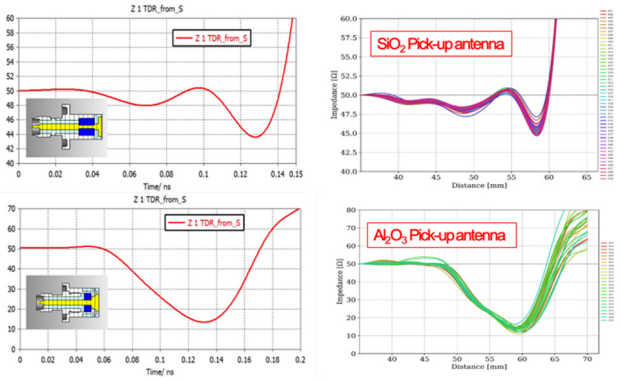


Figure 2: A proto-type of 4GSR BPM pick-up time domain reflection measurements results.

By using TDR data, the capacitance of the BPM pickup electrodes can be estimated through the analysis of the reflected signals. The time-domain reflectometry data provides the necessary information to calculate the capacitance C using the following relation: $C = \Delta t/Z_0$. Here, $\Delta t$ refers to the time delay between the transmitted and reflected signals, and $Z_0$ represents the characteristic impedance of the transmission line.

Through TDR simulations, the expected capacitance for the $SiO_2$ BPM pick-up is approximately 1.5 pF, while the $Al_2O_3$ BPM pick-up is expected to have a capacitance of around 4 pF. The $SiO_2$ BPM pick-up showed good agreement between the simulation and measurement results, with a small standard deviation. However, as shown in Fig. 2, while the $Al_2O_3$ BPM pick-up meets the required impedance and capacitance specifications, the complex manufacturing process and challenges in high-precision

ISBN: 978-3-95450-249-3 ISSN: 2673-5350 doi: 10.18429/JACoW-IBIC2024-TUP30

tolerance machining resulted in a wider range of standard deviation in the measurement results. This could pose difficulties in quality control during mass production. Therefore, we are considering either reestablishing the $Al_2O_3$ BPM pick-up manufacturing process or planning mass production using the $SiO_2$ BPM pick-up. Additionally, by performing TDR measurements on the pick-up antenna, cables, and connectors, and grouping four units with similar phase differences into a single set, the phase difference between the BPM and electronics can be minimized, ensuring consistent beam position data.

Figure 3 shows the final designs of the two types of antennas and fabricated prototypes of the antennas. The $SiO_2$ antenna was manufactured by Kyocera in Japan, while the $Al_2O_3$ antenna components were processed by a domestic company, and brazing was performed at the Pohang Accelerator Laboratory.

Figure 3: The final designs of the two types of antennas completed through optimization, as well as the prototypes of the antennas. The $SiO_2$ antenna is shown at the top, and the $Al_2O_3$ antenna is shown at the bottom.

## TEST BPM FOR BEAM TEST AT PLS-II STORAGE RING

We plan to conduct actual beam tests using the prototype antennas in the PLS-II storage ring at the Pohang Accelerator. However, if we reduce the inner diameter of the beam pipe, as in the 4GSR design, the significant difference in inner diameter compared to the PLS-II storage ring beam pipe could lead to an increase in impedance and beam instability. Therefore, it was ultimately decided to manufacture and install a new test BPM to match the specifications of the dummy chamber in the ID straight section of cell 7.

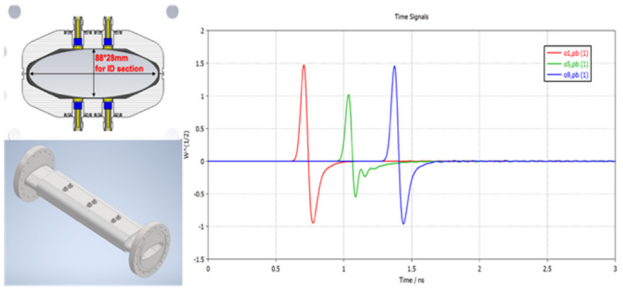


Figure 4: The cross-sectional view and full view of the dummy chamber, and the expected signal output waveform from the three test BPM.

Figure 4 shows the cross-sectional view and full view of the dummy chamber, and the expected signal output waveform from the test BPM was calculated through CST simulations. It was calculated that the $SiO_2$ antenna generates approximately 50% stronger output signals compared to the $Al_2O_3$ antenna. A total of 12 BPM pick-up antennas were installed in the dummy chamber, with the arrangement in the beam direction being $SiO_2$, $Al_2O_3$, and $SiO_2$ antennas, in sets of three. The distance between each BPM pick-up is 10 cm.

To compare the expected results for the 4GSR with the measurement results from the PLS-II beam tests, it is essential to analyze the key parameters of both storage rings. Table 1 presents a comparison of the major parameters between the third-generation storage ring, PLS-II, and the fourth-generation storage ring, 4GSR.

Table 1: Main Parameters of PLS-II & 4GSR of SR

| Parameters [unit] | PLS-II | 4GSR |
|---|---|---|
| Energy [GeV] | 2.5 | 4 |
| Circumference [m] | 281.82 | 799.297 |
| RF frequency [MHz] | 499.941 | 499.593 |
| Beam current [mA] | 300 @ Beam test | 400 |
| Harmonic number | 470 | 1332 |
| Rev. frequency [MHz] | 1.06 | 0.375 |
| Bunch Length [ps] | 25 | 3.66/14.66 |

## BEAM TEST RESULTS OF TEST BPM FOR 4GSR BPM

### *Raw BPM Signal Measurements*

To evaluate the performance of the 4GSR BPM, test BPMs were installed in the ID straight section of Cell 7 in the PLS-II storage ring at the Pohang Accelerator Laboratory. A total of 12 BPM pick-ups, arranged in three sets, were mounted on the test BPM, with $SiO_2$ pick-ups placed on both sides and an $Al_2O_3$ BPM placed in the center. During the beam tests, the beam current was maintained at 300 mA with top-up operation, and the bunch length in the storage ring was approximately 7.5 mm. The output signals from the BPMs were observed without loss using a high-performance oscilloscope with a 16 GHz bandwidth and 50 GS/s sampling rate to capture the raw waveform. Turn-by-turn (TbT) data for beam position resolution measurements were acquired using I-Tech's Libera Brilliance+ system.

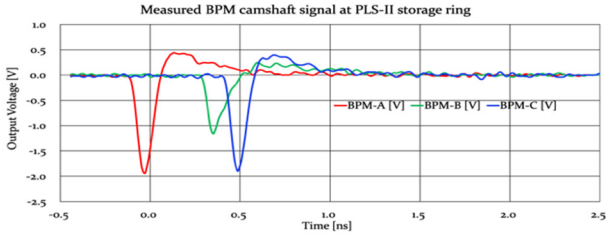


Figure 5: A measured raw BPM signal with test BPM at the PLS-II storage ring.

ISBN: 978-3-95450-249-3 ISSN: 2673-5350 doi: 10.18429/JACoW-IBIC2024-TUP30



Figure 5 shows that a measured raw BPM signal for three test BPM at the PLS-II storage ring. The signal was camshaft signal, which is single bunched beam with high bunch charge in the hybrid beam operation of PLS-II storage ring.

The distance between the BPMs is 10 cm, resulting in a time difference of approximately 0.333 ns between the BPM output signals. However, in this experiment, phase matching was performed only for the four cables set for each BPM, and no phase matching between the BPM cables was carried out. Therefore, the signal spacing is not exactly 0.333 ns due to the cable delay, but the phase difference between each BPM cable set was measured to be consistent with the TDR measurement values.

## *TbT BPM Data Acquisition*

The beam position resolution was measured using the Libera Brilliance+ system. Before performing the beam tests, the Libera Brilliance+ was synchronized by decoding the master oscillator signal and trigger from the 7th cell of the PLS-II storage ring. It was confirmed that the three BPMs were synchronized through the BPM electronics. Based on this, 1000 turn-by-turn data points were collected and repeated 3500 times. This allowed for the measurement of beam position resolution, capturing not only the stabilized beam orbit in the storage ring but also beam orbit data during top-up injection. Figure 6 shows the turn-by-turn data over 3.5 million turns. Beam position oscillations due to top-up injection can be observed in both the X and Y directions, and the sum signal allows for relative observation of the top-up current.

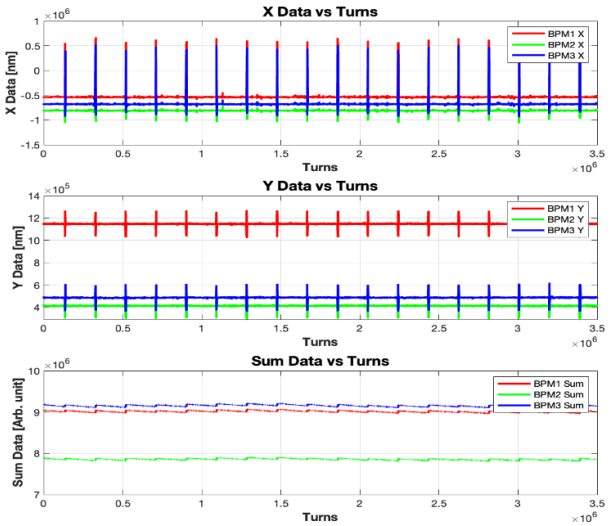


Figure 6: Turn by Turn data during 3.5 million turns with top-up operation.

After acquiring TbT data, the standard deviation of the beam trajectory in both the X and Y directions was calculated to assess the stability of the beam trajectory. In this beam test, the offset of the test BPM was not measured, and since the BPMs were installed as replacements in the dummy chamber of the ID straight section, it was also difficult to perform BBA (Beam-Based Alignment). Therefore, the measured beam positions include offsets. Additionally, the calibration factor used in the beam test was obtained from 3D calibration simulations. Figure 7 shows the histogram of the X and Y data measured over 3.5 million turns. All three test BPMs exhibit similar standard deviation values, with a standard deviation of approximately 12.8 μm in the X direction and 4.7 μm in the Y direction.

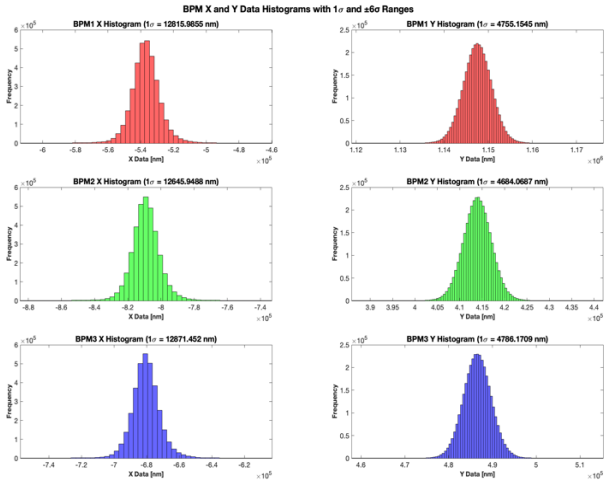


Figure 7: A histogram of TbT X and Y data for checking the orbit stability of the three test BPMs at PLS-II.

## *Beam Position Resolution Measurements Using TbT BPM data*

The data measured from the BPM is essential for ensuring the stability and performance of the accelerator system, and the accuracy of the beam position resolution is one of the key metrics for evaluating this [4-7]. In this study, we conducted a beam position resolution test using three test BPMs. TbT beam position data was acquired through time-domain processing, and the beam position resolution was measured considering the geometrical factor since the three BPMs were installed 10 cm apart. The method used to measure the beam position resolution involved a linear regression-based SVD approach, where the difference (residual) between the predicted and measured values from the BPM was calculated to analyze the position resolution.

For the regression analysis, the X, Y, and SUM data of each BPM were used to predict the beam position at a specific BPM. The predicted value was then compared with the actual measured value, and the final resolution of each BPM was evaluated by performing a geometrical correction. The following equation (Eq. 2) shows how the expected position of BPM-AX was calculated using the linear regression approach:

$$\begin{aligned}\mathrm{BPM-AX\,(predict)} = {} & \alpha 1 \cdot \mathrm{BPM-AY} + \alpha 2 \cdot \mathrm{BPM-BX} + \alpha 3 \cdot \mathrm{BPM-BY} + \alpha 4 \cdot \mathrm{BPM-CX} + \alpha 5 \cdot \mathrm{BPM-CY} + \alpha 6 \cdot \mathrm{BPM-A\_SUM} + \alpha 7 \cdot \mathrm{BPM-B\_SUM} + \\ & \alpha 8 \cdot \mathrm{BPM-C\_SUM}. \qquad (2).\end{aligned}$$

Since this is a button BPM, the beam positions in the X and Y directions are correlated, and although the beam current has a smaller influence, it still affects the beam position. Therefore, this data was used to calculate the

ISBN: 978-3-95450-249-3 ISSN: 2673-5350 doi: 10.18429/JACoW-IBIC2024-TUP30

predicted beam position. After calculating the expected beam position, the residual value (Eq. 3) was obtained by comparing it with the actual measured beam position,

$$Residual = BPM_{AX}(meas.) - BPM_{AX}(pred.). \quad (3).$$

By calculating the RMS value of the residual and applying geometrical factor (G. F.) to each BPM, the actual beam position resolution of each BPM can be measured (Eq. 4),

$$\sigma_{resolution} = \sigma_{residual} \times G.F. \quad (4).$$

This approach provides a systematic way to estimate the beam position resolution using a combination of linear regression and SVD, along with geometrical corrections based on the BPM placement and system layout.

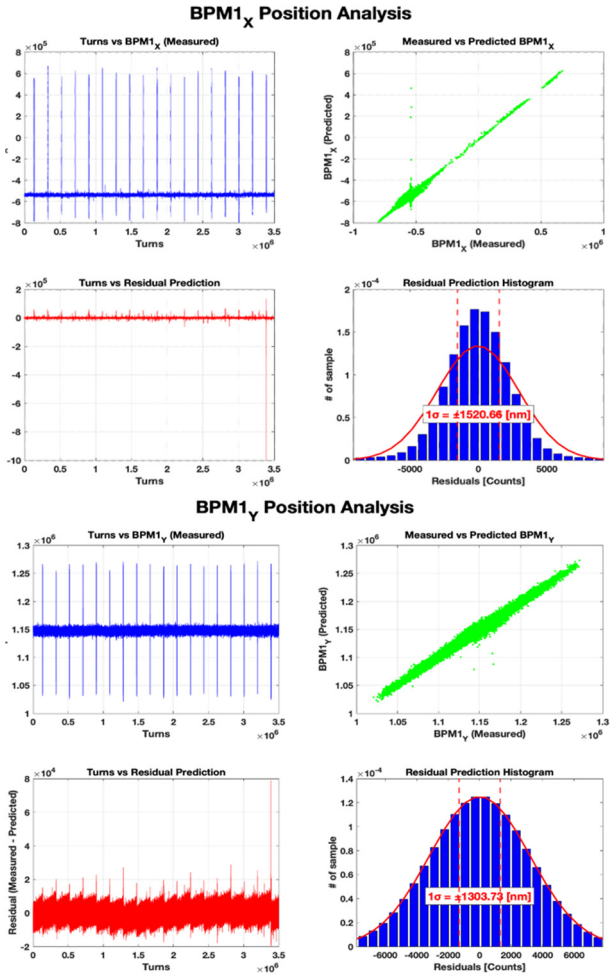


Figure 8: A measured BPM-A resolution with 3.5 million TbT data by using Libera Brilliance+ Time Domain Processing.

Figure 8 shows the result of the resolution measurement with TbT data and 300 mA top-up mode operation. The top left of each subfigure shows the measured beam position at BPM-AX and AY, while the top right compares the measured position with the predicted position for BPM-AX and AY. The bottom of each figure displays the calculated residual (bottom left) and the distribution of the residuals (bottom right). Based on these measurements and analyses, the beam position resolutions for the three BPMs are summarized in Table 2. For the SiO2 BPM, resolutions of approximately 1.5 μm in the X direction and 1.3 μm in the Y direction were achieved, while for the Al2O3 BPM, resolutions of 2.7 μm in the X direction and 2.16 μm in the Y direction were obtained.

Table 2: Measured Three BPM Resolution Results

| BPM resolution | BPM-A ($SiO_2$) | BPM-B ($Al_2O_3$) | BPM-C ($SiO_2$) |
|---|---|---|---|
| X-port [μm] | 1.52 | 2.70 | 1.50 |
| Y-port [μm] | 1.30 | 2.16 | 1.08 |

## CONCLUSION

The Korean 4GSR project in Ochang is currently under construction with the goal of completion by 2027. We developed a prototype of the pick-up antenna for the 4GSR BPM and performed TDR measurements and beam position resolution tests at the PLS-II storage ring using a test BPM chamber designed for this purpose. By utilizing TbT data, we measured beam position resolutions ranging from approximately 1 to 3 micro-meters. Based on the results of the beam test, we will finalize the design of the 4GSR BPM's pick-up antenna and aim to start mass production, targeting completion by 2027.

## ACKNOWLEDGEMENTS

This research was supported in part by the Korean Government (MSIT: Ministry of Science and ICT) (No. RS-2022-00155836, Multipurpose Synchrotron Radiation Construction Project) and also supported by Pohang Accelerator Laboratory (PAL). PAL is supported by Korean Government (MSIT) and POSTECH.

## REFERENCES

[1] G.S. Jang *et al.*, "Low Emittance Lattice Design for Korea-4GSR", *Nucl. Instrum. Methods Phys. Res., Sect. A*, vol. 1034, p. 166779, 2022. doi:10.1016/j.nima.2022.166779

[2] S.-W. Jang and G. Hahn, "Development of beam position monitor for korea 4GSR project", in *Proc. IPAC'23*, Venice, Italy, May 2023, pp. 4832-4835. doi:10.18429/JACoW-IPAC2023-THPL154

[3] CST is an electromagnetic field simulation software, http://www.3ds.com

[4] S. W. Jang, A. Heo, J. G. Hwang, E.-S. Kim, H.-S. Kim, and H. K. Park, "Test Results on Beam Position Resolution for Low-Q IP-BPM at KEK-ATF2", in *Proc. IPAC'11*, San Sebastian, Spain, Sep. 2011, paper TUPC118, pp. 1293-1295.

[5] S. W. Jang *et al.*, "Development of a Low- Q Cavity-Type Beam Position Monitoring System", *IEEE Trans Nucl. Sci*, vol. 64, no. 8, pp. 2353-2360, Aug. 2017. doi:10.1109/TNS.2017.2718033

[6] S. W. Jang, E.-S. Kim, Y. Honda, T. Tauchi, and N. Terunuma, "Development of a Cavity-Type Beam Position Monitors with High Resolution for ATF2", in *Proc. IPAC'13*, Shanghai, China, May 2013, paper MOPME058, pp. 604-606.

[7] G. Kube, J. Neugebauer, and F. Schmidt-F?Âhre, "BPM Resolution Studies at PETRA III", in *Proc. IBIC'19*, Malmö, Sweden, Sep. 2019, pp. 517-521. doi:10.18429/JACoW-IBIC2019-WEPP005